Growth of Trigonal-shaped TiN Nanocrystals via the Metal-catalyzed Reduction-Nitridation Route at Low Temperature

Xuchu Ma, Zude Zhang,* Xuebing Li, Shutao Wang, Yi Du, Fen Xu, and Yitai Qian
Structure Research Laboratory and Department of Chemistry, University of Science and Technology of China,
Hefei, Anhui 230026, P. R. China

(Received January 15, 2004; CL-040058)

Pure trigonal-shaped TiN nanocrystals with the size of 30–50 nm were synthesized from a metal-catalyzed reduction-nitridation (MCRN) route at 350 °C for 6 h, which used $TiCl_4$ and $NaNH_2$ as the starting materials and Mg metal as the catalyst. The obtained sample was characterized by XRD, TEM, and XPS. The effect of the metallic catalyst on the formation of the trigonal-shaped TiN nanocrystalline was discussed.

Titanium nitride is a technologically important material that exhibits excellent chemical stability, low friction coefficient, extremely high hardness, good wear resistance, and electrical conductivity as well as superconductivity.[1,2] The nitride, therefore, finds use in a number of applications such as coatings on cutting tools, microelectronic devices, diffusion barrier, and decorative materials in semiconductor device technique.[3] Generally, TiN powder can be synthesized by the reaction of metal powder or metal hydrides with nitrogen, a mixture of nitrogen and hydrogen, or ammonia at elevated temperatures, the reaction of metal tetrachloride ($TiCl_4$) with ammonia,[4,5] direct nitridation of TiO_2,[6] and rapid solid-state metathesis (SSM) reaction.[7] Recently, the benzene-thermal route and reduction-nitridation synthesis of reaction have been exploited to produce TiN nanocrystals.[8,9] However, most of these reactions involve relative high temperature, which results in the grain growth of the films and powders.

Herein, we describe the use of the reaction between $TiCl_4$ and $NaNH_2$ at 350 °C in autoclave to prepare the trigonal-shaped TiN nanocrystals, in which metal Mg acts as the catalyst. In this work, pure TiN nanocrystals have been successfully obtained at relative low temperature and, furthermore, the as-prepared TiN has a uniform trigonal shape.

All of the manipulations were carried out in a dry glove box with flowing nitrogen gas. In a typical process, 2-mL $TiCl_4$, 3.0-g $NaNH_2$, and 0.144-g Mg metal particles were put into an autoclave of 10-mL capacity. The autoclave was sealed and maintained at 350 °C for 6 h, then cooled to room temperature on standing. The product was collected and washed with 0.1 M hydrochloric acid solution and distilled water, respectively. Finally, the brown-black product was dried in vacuum at 50 °C for 3 h.

The XRD[10] pattern corresponding to powders with random orientation is shown in Figure 1. All of the peaks in Figure 1 could be indexed as a cubic NaCl-typed TiN. Refinement reveals that the cell contains lattice parameters: $a = 4.226$ Å, which is consistent with the literature values (JCPDS cards No. 38-1420: $a = 4.241$ Å).[11] No other impurity, such as TiO_2, could be detected. The broadening nature of the peaks indicates that the sample is nanocrystalline.

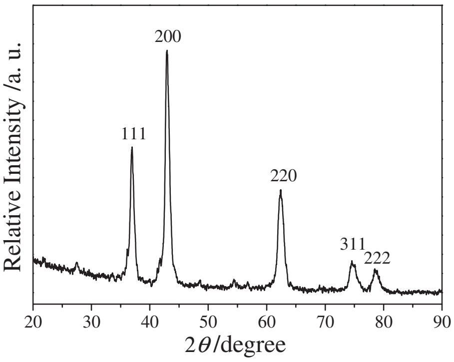

Figure 1. XRD pattern of the as-prepared cubic TiN nanocrystals.

Figure 2 shows the TEM[10] micrograph of the sample as well as the corresponding selected area electron diffraction (SAED) pattern. The TEM (Figure 2a) image reveals that the obtained TiN samples have uniform trigonal shape with the size of 30–50 nm. The SAED (Figure 2b) pattern clearly shows the single crystalline nature of the sample. And the diffraction dots can be indexed as (111), (200), and (311) planes of cubic TiN, which confirms the XRD results.

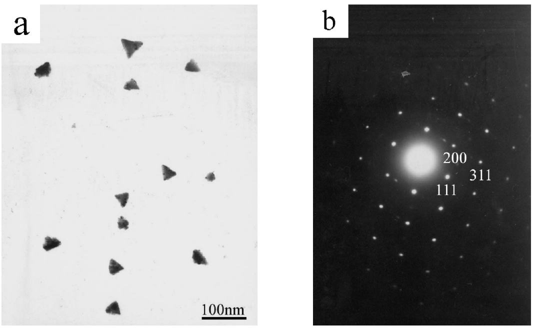

Figure 2. (a) TEM image of the trigonal-shaped TiN nanocrystals and (b) the corresponding selected-area electron diffraction (SAED) pattern.

The XPS[10] spectra (Figure 3) show the composition and the purity of trigonal-shaped TiN nanocrystals. The survey spectrum (Figure 3a) indicates the presence of Ti and N elements, as well as C from the reference and O impurity from absorbed molecules O_2 and H_2O. The binding energy of $Ti_{2p3/2}$ and N_{1s} are 456.30 and 397.05 eV (shown in Figures 3b and 3c), respectively, which are in good agreement with the data of TiN in the literature.[8,12] In addition, the peak corresponding to $Ti_{2p3/2}$ of Ti–O is observed at about 457.80 eV, but no characteristic peaks of TiO_x are observed in the XRD patterns. This observation indicates that the inner bulk phase is pure cubic-phase TiN as confirmed by

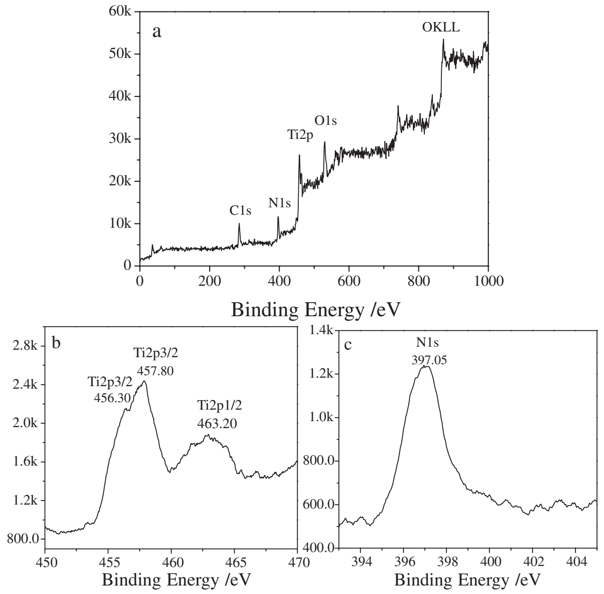

Figure 3. XPS spectra of the trigonal-shaped TiN nanocrystals: (a) a typical XPS survey spectrum of TiN; (b) close-up survey for $Ti_{2p3/2}$ core; (c) close-up survey for N_{1s} core.

XRD measurement, but the surface absorbed many O_2 and H_2O molecules because of the high specific surface area of TiN.

Our approach to the trigonal-shaped TiN nanocrystals is essentially based on the reaction between $TiCl_4$ and $NaNH_2$. It is well known that $NaNH_2$ would decompose to Na_3N by loss of ammonia on heating,[13] and the newly formed Na_3N would also decompose to Na and N_2 when the temperature is higher than 335 °C.[14] Meanwhile, the newly formed NH_3 would also decompose to N_2 and H_2 on this condition. The nascent Na has much higher reductive ability so that $TiCl_4$ could be reduced to Ti by the aid of the reducing agent Na, then Ti is rather reactive toward nitrogen at the elevated temperatures, and an irreversible reaction between Ti and N_2 can easily occur.[14,15] Herein, the Na_3N could be regarded as the intermediate nitrogen source, and the nascent N_2 could be regarded as the final nitrogen source that reacts with Ti to form cubic TiN. The total reaction involved here is as follows:

$$\begin{aligned} TiCl_4(l) + 4NaNH_2 &\xrightarrow{623\,K,Mg} \text{cubic TiN} + 4NaCl \\ &\qquad + \frac{3}{2}N_2(g) + 4H_2(g) \end{aligned}$$

Furthermore, according to free energy calculation, the reaction between $TiCl_4$ and $NaNH_2$, described as the total equation, is thermodynamically driven to the right side and highly exothermic ($\Delta_r G^{\ominus} = -204.26\,\text{kcal}\cdot\text{mol}^{-1}$, $\Delta_r H^{\ominus} = -152.64\,\text{kcal}\cdot\text{mol}^{-1}$). As to the role of Mg, it could be attributed that metal Mg works as a catalyst to favor the reaction proceeding. In the comparison experiments, the XRD results (not shown) demonstrate that no cubic TiN crystals could be obtained at 350 °C, even at 400 °C in the absence of the catalyst Mg. Furthermore, even though TiN can be obtained at 450 °C, the aggregated TiN particles rather than the uniform trigonal-shaped TiN would be obtained without Mg metal. Although the detailed effect of Mg on controlling the formation of trigonal-shaped TiN is not very clear and the reaction needs to be further investigated, the existence of Mg does have the ability to cause the appearance of trigonal-shaped TiN nanocrystals at a relatively low temperature. Meanwhile, if the reaction time is less than 6 h at a suitable temperature, the reaction would be incomplete, and the pure trigonal-shaped TiN nanocrystals could not be obtained.

In summary, 30–50 nm trigonal-shaped TiN nanocrystals can be successfully synthesized via the metal-catalyzed reduction-nitridation (MCRN) route at 350 °C for 6 h, which uses $TiCl_4$ and $NaNH_2$ as the starting materials and Mg metal as the catalyst. Mg metal plays a crucial role in the formation of the trigonal-shaped TiN nanocrystals. It can be expected that the reasonable formation mechanism may have elicitation for the synthesis of other nitrides, such as VN, NbN, Mo_2N, and so on.

Financial supports from the National Natural Science Foundation of China and Chinese Ministry of Education are gratefully acknowledged.

References and Notes

1 A. Kato and N. Tamari, *J. Cryst. Growth*, **29**, 55 (1975).
2 L. E. Griffiths, M. R. Lee, A. R. Mount, H. Kondoh, T. Ohta, and C. R. Pulham, *Chem. Commun.*, **2001**, 579.
3 I. Kim and P. N. Kumta, *J. Mater. Chem.*, **13**, 2028 (2003).
4 L. E. Toth, “Transition Metal Carbides and Nitrides,” Academic Press, New York (1971).
5 C. C. Addision and B. M. Davies, *J. Chem. Soc. A*, **1969**, 1822.
6 J. G. Li, L. Gao, J. Sun, Q. H. Zhang, J. K. Guo, and D. S. Yan, *J. Am. Ceram. Soc.*, **84**, 3045 (2001).
7 Z. A. Munir, *Am. Ceram. Soc. Bull.*, **67**, 342 (1988).
8 J. Q. Hu, Q. Y. Lu, K. B. Tang, S. H. Yu, Y. T. Qian, G. E. Zhou, and X. M. Liu, *J. Am. Ceram. Soc.*, **83**, 430 (2000).
9 X. G. Yang, C. Li, L. H. Yang, Y. Yan, and Y. T. Qian, *J. Am. Ceram. Soc.*, **86**, 206 (2003), and references therein.
10 XRD pattern measurements were carried out on a Philip X’ Pert PRO SUPER rA rotation anode with Ni-filtered Cu Kα radiation ($\lambda = 1.54187$ Å) at 25 °C. TEM image and SAED pattern were taken on a Hitachi Model H-800 instrument with a tungsten filament, using an accelerating voltage of 200 kV. XPS spectra were recorded on a VGESCALAB MKII X-ray photoelectron spectrometer. XPS data were collected in the constant analyzer energy (CAE) made at 20 eV with Mg Kα ($h\nu = 1253.6$ eV) radiation as the excitation source.
11 Powder Diffraction File No. 38-1420. International Centre for Diffraction Data, Newtown Square, PA.
12 “Handbook of Chemistry and Physics,” ed. by R. C. Weast, CRC Press, Boca Raton, FL (1987).
13 F. Xu, X. Zhang, W. Xi, J. Hong, and Y. Xie, *Chem. Lett.*, **32**, 600 (2003), and references therein.
14 “Series of Inorganic Chemistry, Vol. 1, Nobel Gas, Hydrogen, and Alkali Metal,” ed. by G. X. Feng, X. Y. Huang, P. W. Shen, L. H. Zhang, Y. L. Liu, and D. H. Ren, Ke-Xue Press, Chinese (1998).
15 “Advanced Inorganic Chemistry,” 3rd ed., ed. by F. A. Cotton and G. Wilkinson, John Wiley & Sons, Inc. (1972).